ARCHIVES OF ELECTRICAL ENGINEERING VOL. 67(1), pp. 165–177 (2018)

DOI 10.24425/118999

Research on interaction of APFs based on relative gain array

XINGTIAN FENG[1], TIANTIAN SUN[2], WENZHONG MA[1]

[1] *College of Information and Control Engineering*
China University of Petroleum (East China)
66 West Changjiang Road, Huangdao District, Qingdao, China

[2] *Dongying Power Supply Company*
State Grid Shandong Electric Power Company
66 West Changjiang Road, Huangdao District, Qingdao, China
e-mail: topfxt@163.com

(Received: 03.03.2017, revised: 01.03.2018)

Abstract: Different APFs (Active Power Filter) interact with each other when multiple APFs are connected to the grid, and the interactions deteriorate the control performance of APFs and even lead to system instability. This paper presents a method to analyze the dynamic interaction of multiple APFs in a weak grid. This method uses the Norton equivalent principle to establish the mathematical model of a single APF. The mathematical model of the multiple APFs connected to the grid is set up based on the single APF mode. The RGA (Relative Gain Array) principle is used to analyze the interactions among multiple APFs. Besides, this paper analyzes the effect of changing circuit parameters and controller parameters on the change of the interactions. The strategy of weakening and eliminating the interaction is proposed based on rational selection and combination of parameters. Analysis, along with time domain simulation and experimental results, is presented to verify the feasibility and effectiveness of the proposed method and strategy.

Key words: interaction effect, relative gain array, active power filter, Norton equivalent, LCL filter

1. Introduction

As one of the DFACTS (Distribution Flexible AC Transmission System) equipment items, an APF is an effective equipment to suppress the harmonic current in a distribution network. In some cases, multiple APFs are often used in the same distribution network and interactions between different APFs may emerge [1–2]. In the weak network, the interaction cannot be ignored because of its negative effect. This negative interaction effect can lead to the reduction of APF

control performance, the harmonic current cannot be compensated to the maximum extent, and the stability of the system may be destroyed.

There are many researches on the interaction effects of FACTS (Flexible AC Transmission System) in a transmission system, which include interactions of different control loops in the same equipment, interactions in the same type and different types of equipment and so on [3–7]. For example, the Gram determinant analysis method is used in [4] to analyze the interactions between the TCSC (Thyristor Controlled Series Capacitor) and SVC (Static Var Compensator) in a transmission system, which proves that the interactions between the TCSC and SVC are related to the electrical distance of the devices. [5] uses an RGA analysis method to study the interactions between STATCOM (STATic synchronous COMpensator) and the SVC, which shows that the short circuit capacity and the distance between the devices directly affect their interactions. Currently there is little research on the interactions among the DFACTS devices [8–10], and there is no specific analytical methods and solutions.

In this paper, the dynamic interactions among multiple APFs in a distribution network are studied by taking the weak network. First of all, the mathematical model of a single APF is established by using the Norton equivalent principle and then it is used in the distribution system with multiple APFs. After the transfer function of the multi-input and multi-output systems is calculated, an interaction effect among multiple APFs control circuits is analyzed by using an RGA principle. Besides, the effects of changing circuit parameters and controller parameters on changing negative interaction are also studied. This is useful to solve the problem of initial planning and design of the controller. It's also suitable for a stable working condition. At last, the feasibility of the proposing method and its strategy is verified by time domain simulation and experimental results.

2. System mathematical model

2.1. APF mathematical model

In order to achieve better performance of suppressing switching frequency harmonics, the LCL filter is adopted in the APF [11–12]. Compared with the L and LC filters, the LCL filter has better high frequency attenuation in the same inductance, but its control is more complex [13–15]. In this paper, the double closed loop control strategy is proposed, which is based on the inner loop feedback of the capacitor current and the outer loop feedback of the grid connected current. This control strategy can obtain good dynamic performance and load adaptability. The block diagram of a single APF using the LCL filter and double closed loop control structure is shown in Fig. 1(a).

In Fig. 1(a), the current control loop adopts a PI regulator, which ensures that the output filter current follows a given reference harmonic current i_{ref}. i_{ref} is the harmonic content which extracts from a load current by the Park transform. The inverter adopts bipolar SPWM modulation and it can be equivalent to a controlled voltage source as shown in Fig. 1(b). G_{si} is the current controller; G_{pwm} is the transfer function of the modulator input to the output of the inverter; H_{i1} and H_{i2} are the feedback coefficient of the inner loop and the external loop respectively. From Fig. 1(b), it

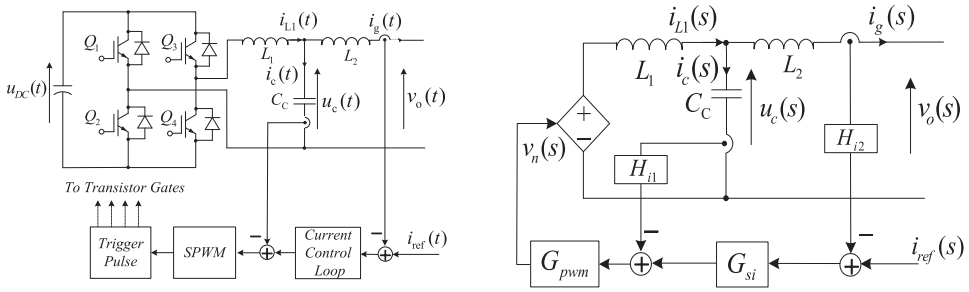

(a) Block diagram (b) Simplified block diagram

Fig. 1. Diagram of an single-phase APF

can be concluded that:

$$\begin{cases} [(i_{\text{ref}} - H_{i2} i_g) G_{si} - H_{i1} i_c] G_{pwm} = \dfrac{1}{sC} i_c + (i_g + i_c) L_1 s \\ i_c = (v_o + i_g s L_2) sC \end{cases} . \tag{1}$$

In order to facilitate the analysis, the APF is treated with the Norton equivalent principle. A short circuit current is obtained by (2).

$$i_{sc}(s) = i_g(s)\Big|_{v_o=0} = \frac{G_{pwm} G_{si} i_{\text{ref}}}{s^3 L_1 L_2 C + s^2 H_{i1} L_2 C G_{pwm} + s(L_1 + L_2) + G_{pwm} G_{si}} = G_i(s) i_{\text{ref}} . \tag{2}$$

Open circuit voltage is obtained by (3).

$$v_{oc}(s) = v_o(s)\Big|_{i_g=0} = \frac{G_{pwm} G_{si} i_{\text{ref}}}{s^2 L_1 C + s H_{i1} C G_{pwm} + 1} . \tag{3}$$

According to (2) and (3), the output impedance z_o of the APF can be achieved.

$$Z_o(s) = \frac{u_o(s)}{i_g(s)} = \frac{s^3 L_1 L_2 C + s^2 H_{i1} L_2 C G_{pwm} + s(L_1 + L_2) + G_{pwm} G_{si}}{s^2 L_1 C + s H_{i1} G_{pwm} C + 1} . \tag{4}$$

The Norton equivalent circuit of the APF is shown in Fig. 2(a). $G_i i_{\text{ref}_i}$ is the controlled current source.

$$i_{gi} = G_i i_{\text{ref}i} - Y_o u_{oi} , \tag{5}$$

$$Y_o(s) = \frac{1}{Z_o(s)} = \frac{s^2 L_1 C + s H_{i1} G_{pwm} C + 1}{s^3 L_1 L_2 C + s^2 H_{i1} L_2 C G_{pwm} + s(L_1 + L_2) + G_{pwm} G_{si}} . \tag{6}$$

By (5) and (6), we can know that the output performance of the APF is related to the parameters of the current loop, the PWM modulator parameters, the LCL filter parameters and the feedback coefficients.

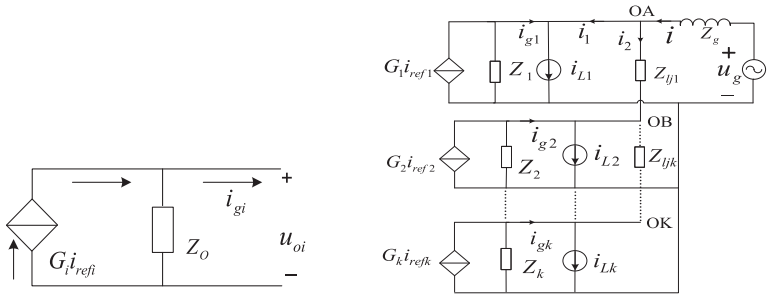

(a) Norton equivalent circuit (b) System structure with multiple APFs

Fig. 2. Equivalent circuit of APF

2.2. Modeling Analysis of multiple APFs connected to the system

An APF is connected to the grid in parallel with the harmonic loads, and the loads are usually nonlinear. Most of the nonlinear loads are equipped with a front-end rectifier, and the modeling is more complicated. In order to facilitate the analysis, the nonlinear loads are simplified as the current sources. The structure of multiple APFs connected to the power system (taking two APFs as an example) is shown in Fig. 2(b).

In Fig. 2(b), i_{L1}, i_{L2} stand for the harmonic load current: Z_{lj1} is the line impedance between the APF1 and APF2 of the weak grid, which we use toreplace Z_{lj} in this paper; u_g is the voltage of the system. From Fig. 2(b), we can obtain as follows:

$$\begin{cases} (u_g - u_{OA})Y_g = i_2 + [i_{L1} - (G_1 i_{\text{ref1}} - Y_1 u_{OA})] \\ i_2 = i_{L2} - (G_2 i_{\text{ref2}} - Y_2 u_{OB}) \\ u_{OB} = u_{OA} - i_2 z_{lj} \end{cases} . \tag{7}$$

When harmonic voltage is the only excitation, the current response of the APF has only a high frequency component. In addition, the system voltage has only a fundamental component, so $u_g = 0$ in the equivalent circuit of the system. We can get (8) according to (7).

$$\begin{cases} u_{OA} = \dfrac{(1+Y_2 z_{lj})(G_1 i_{\text{ref1}} - i_{L1}) - i_{L2} + G_2 i_{\text{ref2}}}{(1+Y_2 z_{lj})(Y_g + Y_1) + Y_2} \\ u_{OB} = \dfrac{G_1 i_{\text{ref1}} - i_{L1} + [1 + Z_{lj}(Y_1 + Y_g)](G_2 i_{\text{ref2}} - i_{L2})}{(1+Y_2 z_{lj})(Y_g + Y_1) + Y_2} \end{cases} . \tag{8}$$

According to (8) and (5), (9) can be obtained as:

$$\begin{bmatrix} i_{g1} \\ i_{g2} \end{bmatrix} = \begin{bmatrix} \dfrac{Y_g(1+Y_2 z_{lj}) + Y_2}{T} G_1 & -\dfrac{Y_1}{T} G_2 & \dfrac{Y_1(1+Y_2 z_{lj})}{T} & \dfrac{Y_1}{T} \\ -\dfrac{Y_2}{T} G_1 & \dfrac{Y_1 + Y_g}{T} & \dfrac{Y_2}{T} & \dfrac{Y_2 + Y_2 z_{ij}(Y_1 + Y_g)}{T} \end{bmatrix} \begin{bmatrix} i_{\text{ref1}} \\ i_{\text{ref2}} \\ i_{L1} \\ i_{L2} \end{bmatrix} . \tag{9}$$

Here: $T = (1 + Y_2 Z_{lj})(Y_g + Y_1) + Y_2$.

When the non diagonal elements of the transfer function matrix in (9) are not zero, it proves that the control circuit is not only controlled by its own loop, but also affected by other control loops. There exist interactions between different control loops. Similarly, we can get a transfer function matrix of m rows and $2m$ columns, when multiple APFs are connected to the grid, and m is the number of the APF.

3. Analysis of interactive effects of multiple APFs and eliminating strategy

According to the above-mentioned mathematical model, the following analysis focuses on the interaction effects and eliminating strategy.

3.1. Analysis of interaction effects based on RGA principle

The RGA matrix can be calculated by (10) if the transfer function $G(jw)$ of the input and output variables is known [16–19]. We can get the RGA matrix of two APFs connected to the system by plugging (9) into (10). The interactive influence of each control loop can be known by analyzing the RGA matrix. We can also analyze the change rule of interaction effects of changing circuit parameters and controller parameters using the RGA matrix.

$$R_{RGA}[G(jw)] = G(jw) \otimes (G(jw)^{-1})^T. \tag{10}$$

In (10), $\otimes$ represents the multiplication of corresponding elements in a matrix, which is the Hadamard product.

The dynamic interaction of two APFs with an LCL filter is studied as an example in this section, in order to seek the relationship between the interaction effect and the controller parameters, the power grid intensity and the electrical distance. In weak grid, the equivalent inductance is 1 mH, the frequency is 50 Hz, and the voltage is 220 V. The parameters of the APFs are shown in Table 1.

Table 1. Parameters of APFs

Equipment	L_1**/mH**	L_2**/mH**	C**/uF**	k_p	K_i	H_{i1}	H_{i2}
APF1	2.7	0.3	4	0.09	300	0.13	1
APF2	3	0.2	3	0.11	400	0.16	1

The block diagram of a single APF with a double closed control loop is shown in Fig. 3(a), and the transfer function of the open loop and closed loop is obtained as (11).

$$\begin{cases} T_{\text{open}} = \dfrac{H_{i2}G_{pwm}G_{si}}{s^3L_1L_2C + s^2L_2CH_{i1}G_{pwm} + s(L_1+L_2)} \\ T_{\text{close}} = \dfrac{G_{pwm}G_{si}}{s^4L_1L_2C + s^3L_2CH_{i1}G_{pwm} + s^2(L_1+L_2) + H_{i2}G_{pwm}G_{si}} \end{cases}. \tag{11}$$

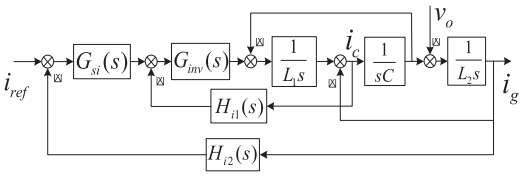

(a) Block diagram with dual-loop control scheme

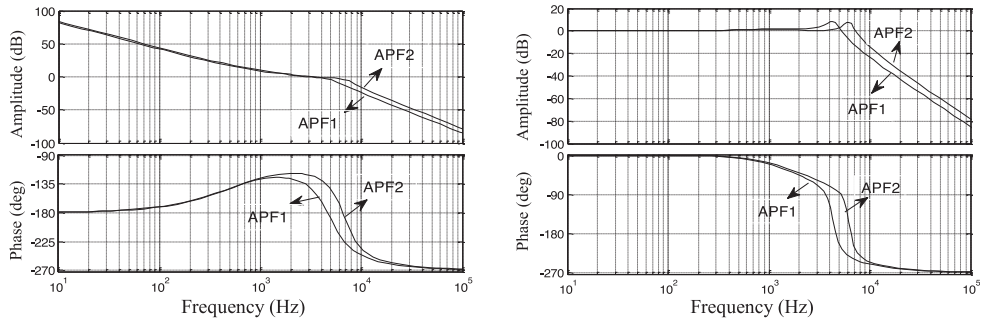

(b) Bode diagram of open loop and closed loop

Fig. 3. Control analysis of an APF

The bode diagram of the open and closed loop transfer function is shown in Fig. 3(b). Two APFs are satisfied with the conventional dynamic stability requirements of phase margin greater than 30° and the amplitude margin greater than 3 dB.

The resonance point of each APF appears above 2 kHz, which is shown in Fig. 3(b). The APFs can keep stable operation in the frequency band below 2 kHz, but the output has a certain error near the APFs resonance point. Therefore, this paper analyzes only the dynamic interaction in the frequency band below 2 kHz.

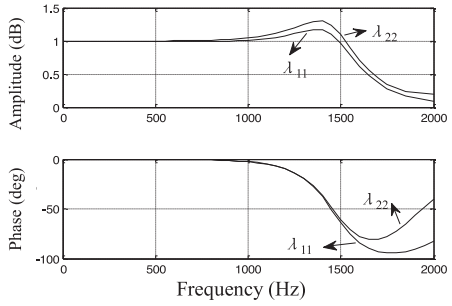

Fig. 4. Analysis of λ_{11}, λ_{22} on different frequency

After entering the data from Table 1 into 10, the RGA matrix can be achieved. Fig. 4 shows the amplitude and phase diagrams of the diagonal elements of RGA matrix λ_{11}, λ_{22}in the frequency band below 2 kHz. As can be seen in the low frequency section below 800 Hz, there is no interactions in the control loops of the two APFs. In a frequency band of 800–1500 Hz, the relative gain is greater than 1. Especially in a band of about 1.4 kHz, the relative gain achieves

minimum. The interaction of the two APFs in the frequency band makes the closed-loop gain of the APF control loop increase, which leads to the control performance reduced and the stability of the system seriously affected. When the frequency is higher than 1.5 kHz, the relative gain is less than 1, and the interaction effect makes the closed-loop gain of the APF greatly reduced, which also affects the control performance of the APF.

Figs. 9 and 10 show that the elements of the RGA matrix are closely related to the parameters of the APF controller, the intensity of the power grid and the electrical distance between the two APFs. Fig. 5 shows the relationship between amplitude as well as phase of the relative gain (taking λ_{11} as an example) and frequency in different APF parameters (K_p, K_i, H_i), power grid intensity (L_g) and the electrical distance between two APFs (L_{lj}).

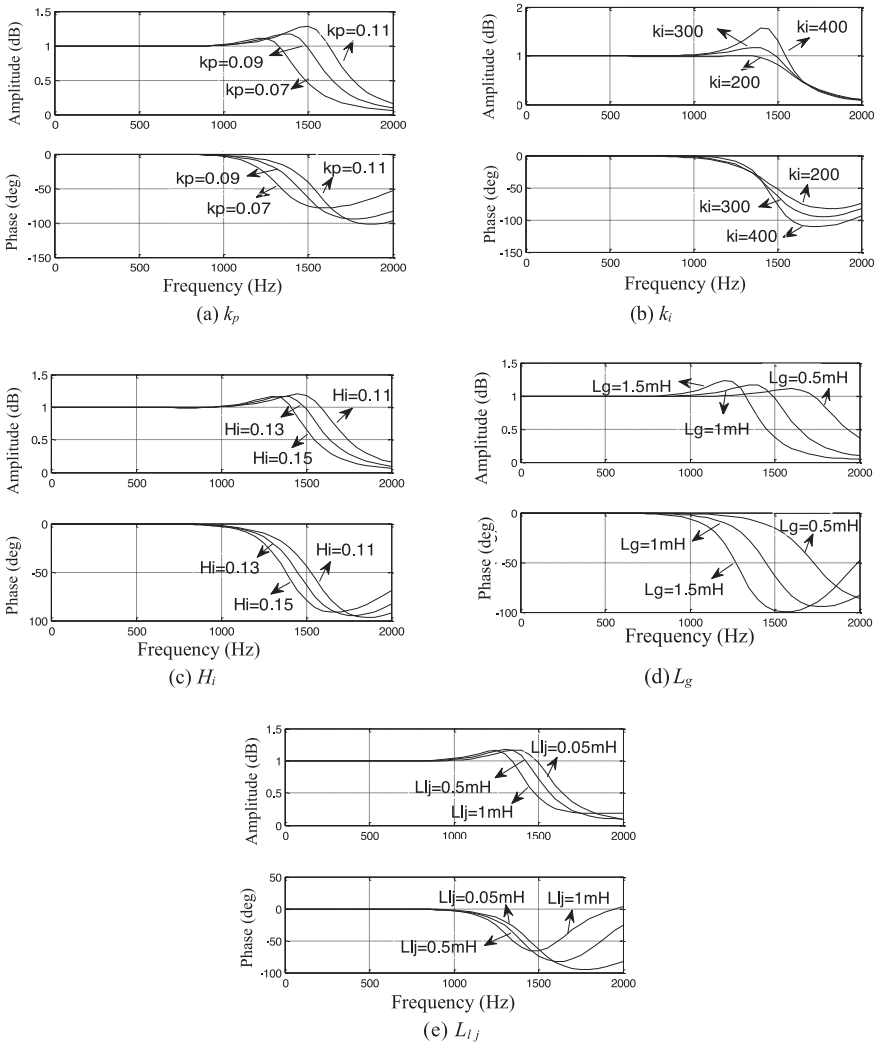

Fig. 5. Effect of APF and grid parameters on λ_{11}

Based on simulation results of Fig. 5, some changing rules of the interactions are concluded. The APF controller parameters, power grid intensity and the electrical distance between different APFs have impact on the relative gain. The relative gain greater than 1 or less than 1 will change the APF closed-loop gain and reduce the compensation performance of the APF, which will affect the stability of the system.

3.2. Simulation verification

Establishing simulation models of a single APF1 and APF1, as well as APF2 connected to the system. Parameters of the two APFs are shown in Table 1. The parameters of the system are the same as the above-mentioned settings. Fig. 6 is a simulation model of the APF1 connected to the grid. Fig. 7 is a simulation model of the APF1 and APF2 connected to the grid.

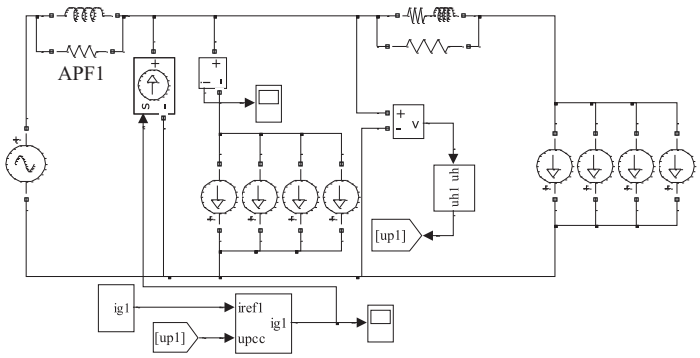

Fig. 6. Simulation model of the APF1 connected to the grid

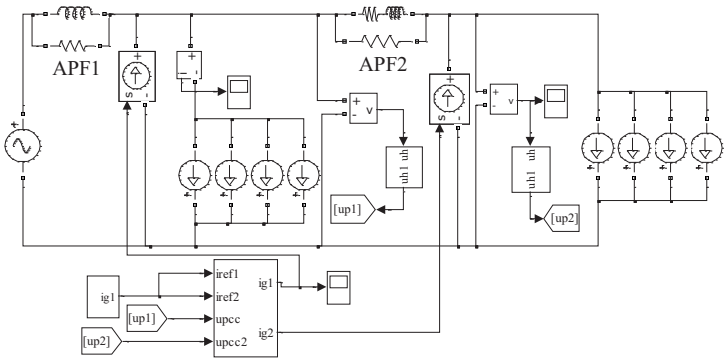

Fig. 7. Simulation model of the APF1 and APF2 connected to the grid

The fundamental reference current is 70A, and harmonic currents (including 5% 600 Hz, 5% 1400 Hz and 5% 1700 Hz) are added in the harmonic load. The content of the APF1 output harmonic currents is shown in Fig. 8 when the APF1 alone, APF1 with APF2 are connected to the grid.

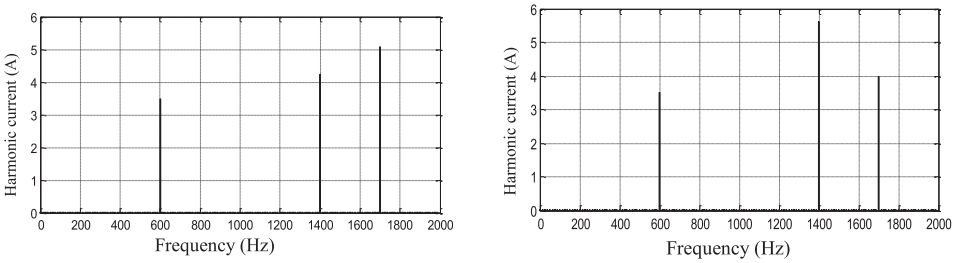

(a) APF1 alone (b) APF1 with APF2

Fig. 8. Harmonic output of the APF1 when connected to the grid

It can be seen from Fig. 8 that the APF2 connected to the grid leads to the increase of the output harmonic current in the APF1 1400 Hz, while 1700 Hz harmonic current is reduced, which is consistent with the theoretical analysis in Fig. 4. Fig. 9 shows that the APF1 outputs harmonic currents when circuit parameters and control parameters change after both the APF1 and APF2 connected to the grid.

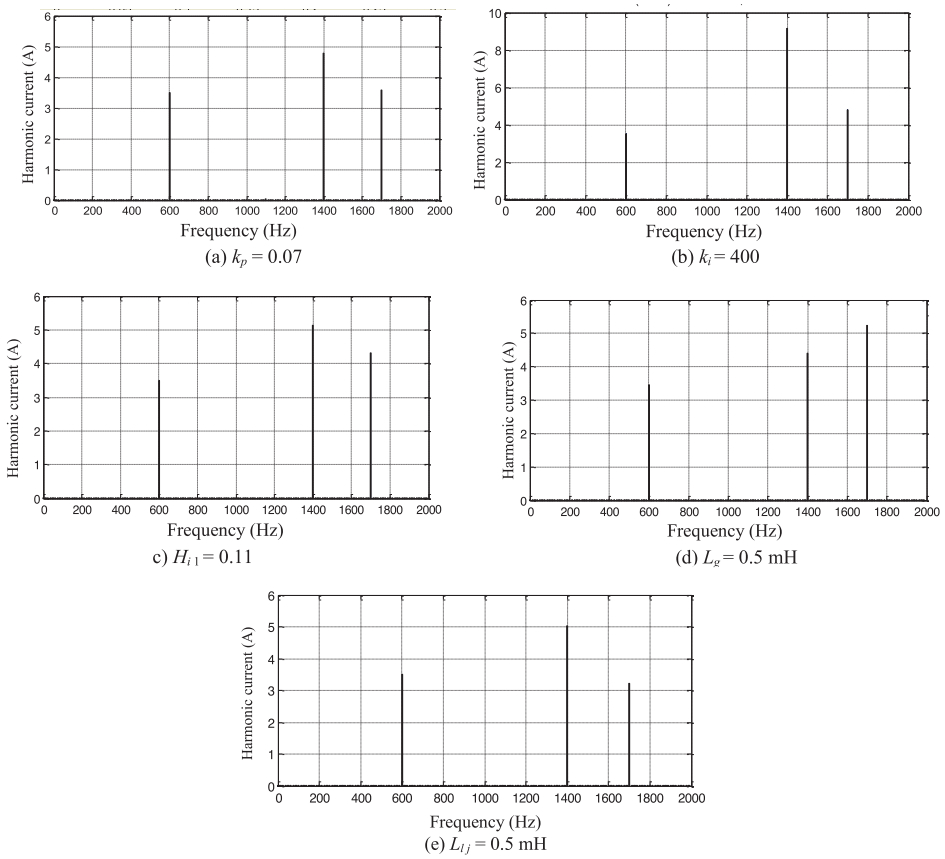

(a) $k_p = 0.07$ (b) $k_i = 400$

c) $H_{i1} = 0.11$ (d) $L_g = 0.5$ mH

(e) $L_{lj} = 0.5$ mH

Fig. 9. Harmonic output of the APF1 when circuit parameters and control parameters changing

Comparing Fig. 8 with Fig. 9, it was seen that the APF1 output harmonic current below 600 Hz is basically invariant no matter how the parameters change. 1400 Hz and 1700 Hz harmonic currents are both reduced when k_p is reduced to 0.07. An output content of 1400 Hz increases, while 1700 Hz remains unchanged, when k_i increased from 300 to 400. Therefore, decreasing k_i can reduce the negative interaction between APFs. When H_{i1} is reduced to 0.11, the 1400 Hz harmonic current is decreased slightly, while 1700 Hz harmonic current becomes significantly larger. When L_g is reduced to 0.5 mH, 1400 Hz harmonic content is reduced, while 1700 Hz harmonic content is increased. 1400 Hz and 1700 Hz harmonics are both slightly decreased as L_{lj} is increased to 0.5 mH. These changes are consistent with the theory analysis in Fig. 5, which verifies the feasibility of this method.

3.3. Strategy of eliminating or reducing the interactions

From the above analysis, we have concluded that the change of each parameter has a certain effect on the relative gain. Reasonable selection and combination of these parameters will reduce or eliminate the negative interaction of multiple APFs in the required frequency. The APF can detect the frequency and content of harmonic currents. According to the relationship between the interaction and frequency in Fig. 4, the influenced frequency of the APF1 affected by the APF2 is determined. Based on Fig. 5 we came to know the rules that change the interactions when applied to the parameters. Therefore, according to these rules, selecting appropriate parameters can reduce the negative interactions. According to Fig. 5(b), for example, smaller k_i helps to reduce the negative interaction when k_i is bigger than 200, so we should select a small value. We need to select parameters by trial and error here as there is no calculation method yet. The method can be a subject of future research. Usually, the number of parameters that need to be adjusted increases, as the number of output harmonic currents increases. The process requires repeated selection and collocation. Two APFs were used as an example to introduce the parameter matching strategy.

The APF1 needs an output harmonic current of 600 Hz, 1400 Hz and 1700 Hz, while the APF2 connected to the grid leads to 1400 Hz harmonic current increase and to 1700 Hz harmonic current reduction. In this case, the following steps are adopted to reduce the interference of the APF1:

(1) According to Fig. 5, changing k_i has little influence on the output of the 1700 Hz harmonic current. Whereas, changing k_i can make an APF1 output of 1400 Hz harmonic current improved. Here, reduce k_i to 250.
(2) Improve the output of the 1700 Hz harmonic current through changing other parameters. Here, reduce H_{i1} to 0.08.
(3) Changing H_{i1} increases the output of 1700 Hz current, while reduces the output of 1400 Hz current. Therefore, modifying k_i again is necessary. Here, increase it to 290. The simulation is carried out after the parameters are modified when the APF1 and APF2 are connected to the grid at the same time. The harmonic current of the APF1 is shown in Fig. 10.

On the basis of Fig. 10, we conclude that, when the APF1 and APF2 are connected to the grid, the amplitude of harmonic current output caused by the APF1 is consistent with a single APF1 connected to the grid after the parameters are corrected. That is to say, parameter selection and coordination can reduce or even eliminate the negative impact on multiple APFs when it is connected to the grid, which proves the feasibility of this strategy.

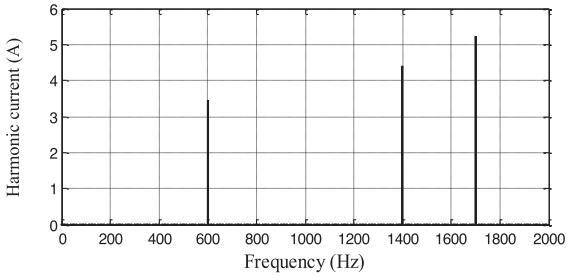

Fig. 10. Harmonic output of the APF1 when parameters changing

3.4. Experimental analysis

In order to verify the effectiveness of the above-mentioned strategy, two 50 kVA three-phase APF prototypes are designed. Table 2 shows the related electrical parameters of the experimental system. Both APFs are in an almost identical environment. Corresponding experimental waveforms and current THD (Total Harmonic Distribution) data are shown in Fig. 11 which takes phase *A* as an example.

Table 2. System electrical parameters

Description	**Real value**
Nominal line voltage	380 V
System frequency	50 Hz
Switching frequency	7.2 kHz
Resistance load	17
Inductance load	46 mH
Nonlinear load	3-phase rectifier + 12 Ω

In Fig. 11, i_{La} is the load current; i_{sa} is the grid current; i_{ca} is the APF output current; i_{sn} is the neutral current in a three-phase four-line system. Figs. 11(a) and (b) show the waveforms before adopting the proposed strategy of eliminating or reducing the interactions. Fig. 11(e) shows the corresponding grid current THD when using the APF1 (left figure) and APF2 (right figure) together. It can be seen that the grid current THD has satisfied the requirement of THD $< 5\%$, but there exists interaction between two APFs according to the above analysis method, especially on the 17^{th} harmonic. Through adopting the proposed strategy of eliminating or reducing the interactions, Figs. 11(c), (d) and (f) show the experimental results. According to Fig. 11(f) (APF1 left, APF2 right), the 17^{th} harmonic is decreased to nearly zero and the grid current THD is lower than in Fig. 11(e). The strategy reduces the interactions and APFs have better filtering effect.

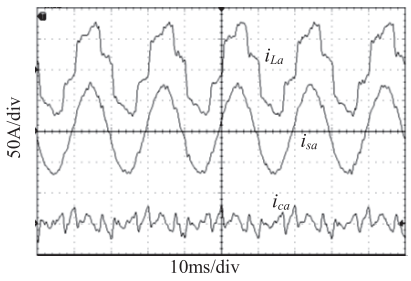

(a) Before adopting strategy of the APF1

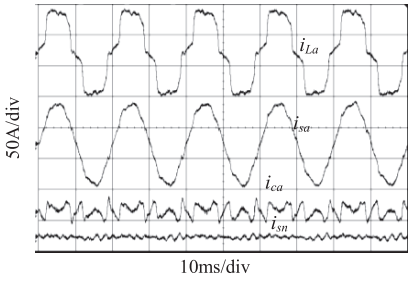

(b) Before adopting strategy of the APF2

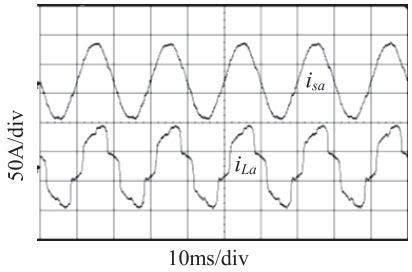

(c) After adopting strategy of the APF1

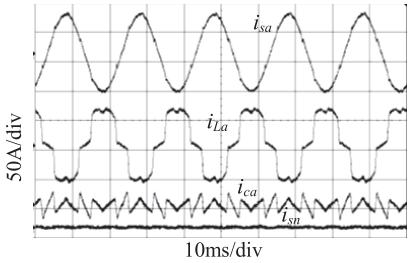

(d) After adopting strategy of the APF2

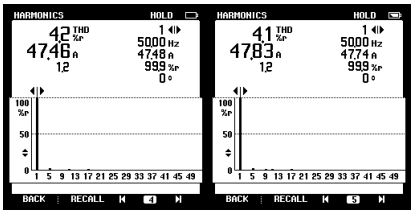

(e) THD before adopting strategy

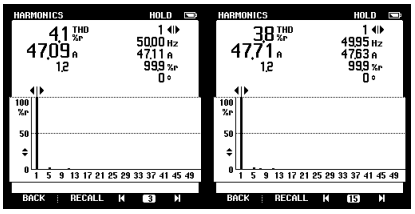

(f) THD after adopting strategy

Fig. 11. Experimental waveforms and THD data

4. Conclusions

In this paper, a mathematical model of multiple APFs connected to the grid is established, and the transfer function model of the multi-input and multi-output system is established to analyze the interaction problems. The dynamic interaction of multiple APFs is analyzed based on the RGA principle. The changing rules of the interaction are studied in detail in the case of changing APF controller parameters, power grid intensity and the electrical distance between two APFs. Reasonable parameter selection and coordination can reduce or even eliminate the negative interaction effect. Time domain simulation and experimental results verify the feasibility of the analysis method and the improvement strategy.

Acknowledgements

This work was supported by Fundamental Research Funds for the Central Universities under Project 18C-X02114A and National Natural Science Foundation of China under Project 51477184 and 51777216.

References

[1] Chu L., Tu C., Luo A., Shuai Z., Chau M., *A series Hybrid APF Design for Integrated Compensation of Different Types of Harmonic Sources*, Automation of Electric Power Systems, vol. 37, no. 8, pp. 123–128 (2013).

[2] Xu C., Zhu Q., Zhang H., *Study of Distributed Photovoltaic Grid-connected Unified Control Strategy of SAPF and Inverter*, Power Electronics, vol. 49, no. 11, pp. 24–28 (2015).

[3] Jiang Q., Zou Z., Wu H., Cao Y., Wang H., *Interaction Analysis of Facts Controllers Based on RGA Principle*, Proceedings of the CSEE, vol. 25, no. 11, pp. 23–28 (2005).

[4] Yang W., Qu Y., Gu M., *Using Gramian to Analyze the Mutual Influence of Power System with FACTS*, Power System Protection and Control, vol. 39, no. 22, pp. 30–34 (2011).

[5] Li F., *Research on the Simulation and Application of STATCCOM in Multi-Machine Power System*, M.S. Thesis, Information Engineering School, Nanchang University, Nanchang (2006).

[6] Farsangi M.M., Song Y.H., Kwang Y.L., *Choice of FACTS devices control inputs for damping inter-area oscillations*, IEEE Transactions on Power Systems, vol. 19, no. 2, pp. 1135–1143 (2004).

[7] Li H., Dong P., Liu M., Xu L., Wang Q., *Analysis on Interaction Between FACTS Devices and HVDC Power Transmission System in China Southern Power Grid Based on Relative Gain Array and Prony technology*, Power System Technology, vol. 36, no. 8, pp. 169–174 (2012).

[8] Chen J., Wang Z., Yao Y., *Study on Interactions of DFACTS Devices Operating in Distribution System*, Electrical Measurement & Instrumentation, vol. 51, no. 9, pp. 50–56 (2014).

[9] Dang P., Ellinger T., Petzoldt J., *Dynamic Interaction Analysis of APF Systems*, IEEE Transactions on Industrial Electronics, vol. 61, no. 9, pp. 4467–4473 (2014).

[10] Jia D.Q., Wei T., Huo Q., *The Interaction Analysis Between AC and DC Control Loop of DSTATCOM*, Transacions of China Electrotechnical Society, vol. 28, no. s1, pp. 324–330 (2012).

[11] Bao C., Ruan X., Wang X., Pan D., Li W., Weng K., *Design of Grid-connected Inverters with LCL Filter Based on PI Regulator and Capacitor Current Feedback Active Damping*, Proceedings of the CSEE, vol. 32, no. 25, pp. 133–142 (2012).

[12] Tang S.Q., *Design and Current Control Strategy of LCL-filter based on Shunt Active Power Filter*, M.S. Thesis, School of Electrical Engineering and Automation, Harbin Institute of Technology, Harbin (2012).

[13] Xu Z., Xu A., Xie S., *Dual-loop Grid Current Control Technique for Grid-connected Inverter Using An LCL Filter*, Proceedings of the CSEE, vol. 29, no. 27, pp. 36–41 (2009).

[14] Twining E., Holmes D., *Grid Current Regulation of a Three-phase Voltage Source Inverter with an LCL Input Filter*, IEEE Transactions on Power Electronics, vol. 18, no. 3, pp. 888–895 (2003).

[15] Fereidouni A., Masoum M.A.S., Smedley K.M., *Supervisory Nearly Constant Frequency Hysteresis Current Control for Active Power Filter Applications in Stationary Reference Frame*, IEEE Power and Energy Technology Systems Journal, vol. 3, no. 1, pp. 1–12 (2016).

[16] Milanovic J.V., Duque A.C.S., *Identification of Electromechanical Modes and Placement of PSSs Using Relative Gain Array*, IEEE Transactions on Power Systems, vol. 19, no. 1, pp. 410–417(2004).

[17] Cai L., Erlich I., *Identification of the Interactions among the Power System Dynamic Voltage Stability Controllers using Relative Gain Array*, 2006 IEEE PES Power Systems Conference and Exposition, Atlanta, Georgia, USA, pp. 970–977 (2006).

[18] Li P., Yang S., Yin Z., *Voltage Stabilization and Decoupling Droop Control Method for Microgrid Based on RGA*, Proceedings of the CSEE, vol. 35, no. 5, pp. 1041–1050 (2015).

[19] Hu W., Sun J., Ma Q., Liu F., Zha X., *Analysis on Interactive Influences Among Multi Grid-Connected Inverters*, Power System Technology, vol. 38, no. 9, pp. 2511–2518 (2014).